A

RNA-seq					
Sample	Total Reads	Mapping rRNA		Mapping genome	
		Mapped reads	% contamination	Mapped (Uniquely)	% (of raw data)
sh-Ctrl_1	81,517,731	3,219,405	3.95	17,130,126	21.88
sh-Ctrl_2	75,204,811	3,316,119	4.41	15,911,405	22.13
sh-UPF1_1	82,630,892	2,898,637	3.51	18,716,052	23.47
sh-UPF1_2	81,568,719	15,628,651	19.16	13,431,650	20.37
sh-eRF3A_1	91,595,387	2,339,477	2.55	17,120,904	19.18
sh-eRF3A_2	67,317,174	1,502,035	2.23	11,389,315	17.31

B

Ribo-seq									
Sample	Total Reads	Trim Adapt (25-34)				Mapping rRNA		Mapping genome	
		Adapter present + size filter ok	%	Too short	Too long	Mapped reads	% contamination	Mapped (Uniquely)	% (of raw data)
sh-Ctrl_1	496,037,564	366,124,433	73.8	5,229,054	10,913,389	45,870,113	12.5	133,733,098	27.0
sh-Ctrl_2	411,820,853	269,795,611	65.5	10,183,184	20,115,833	25,493,141	9.4	114,401,028	27.8
sh-UPF1_1	386,563,970	221,204,420	57.2	6,897,235	13,589,959	49,671,167	22.5	78,854,057	20.4
sh-UPF1_2	444,079,333	309,649,847	69.7	8,880,901	34,570,906	33,528,160	10.8	139,575,763	31.4
sh-eRF3A_1	406,326,972	309,337,455	76.1	9,869,052	14,126,353	40,761,681	13.2	137,032,369	33.7
sh-eRF3A_2	406,058,053	296,980,600	73.1	9,043,793	14,467,973	48,034,296	16.2	136,422,829	33.6

Supplemental Figure S1

Tables summarizing the counting of reads after the different bioinformatic filters in RNA-seq analysis (**A)** and Ribo-seq analysis (**B)**.

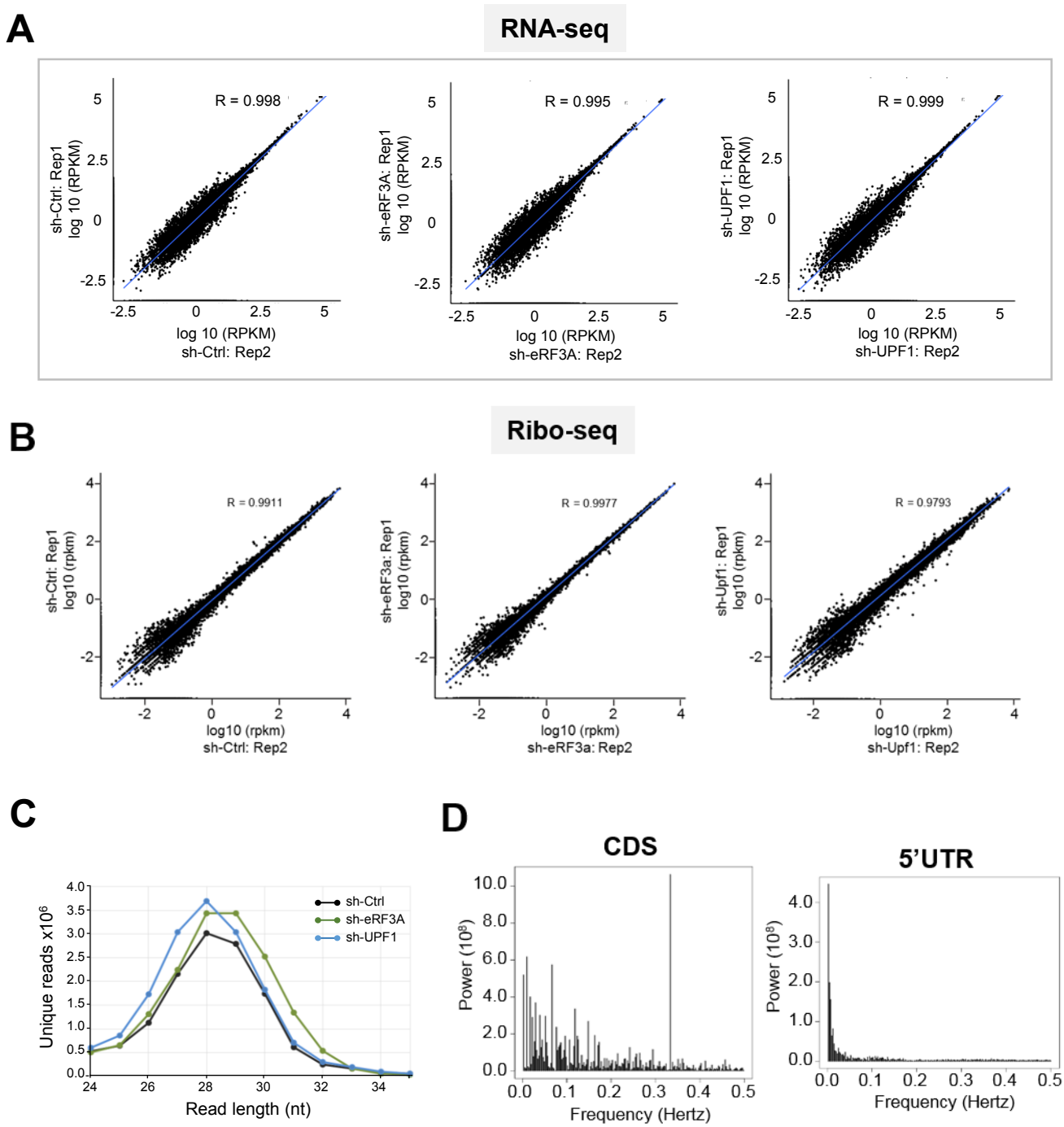

Supplemental Figure S2

Monitoring of RNA-seq ribosome profiling in HCT116 cells. A and **B**. Double-log scatter plots comparing RPKM (reads per kilobase million) between the two biological replicates (Rep1 and Rep2) of RNA-seq (**A**) and ribosome profiling (**B**) experiments carried out on independent libraries sequenced fourth; HCT116 cells expressing sh-Ctrl (left panel), sh-eRF3A (middle panel) and sh-UPF1 (right panel). The Pearson correlation coefficient R is shown for each plot. **C.** Length distribution of ribosome footprint sequences after excluding nuclease-generated rRNA contaminations in control, eRF3A and UPF1 depleted cells. **D.** Periodicity analysis at the 5' end of the read coverage for the coding sequences (**CDS**) and **5'UTR**s. The power spectral density of the signal (Power) was plotted versus the frequency (in Hertz). For the coding sequences (CDS periodogram), the 3-bp periodicity (1/Frequency) is apparent as a peak at 0.3 Hertz.

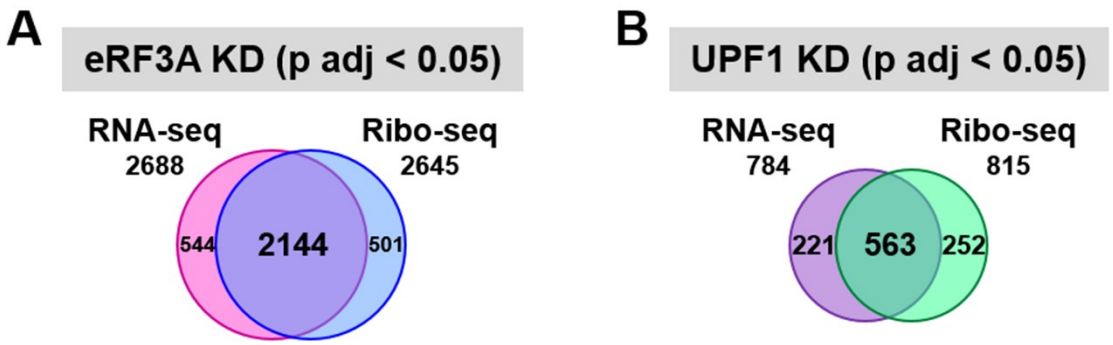

Supplemental Figure S3

Differentially expressed genes in eRF3A and UPF1 knockdown cells. Proportional Venn diagrams showing the overlap of differentially expressed genes (adjusted p-value, p adj < 0.05, DESeq2). For each Venn diagram, the number of genes are indicated. **A.** Comparison of mRNA abundance changes (**RNA-seq**) with main coding sequence changes (**Ribo-seq**) of differentially expressed genes in eRF3A knockdown (**eRF3A KD**) cells. **B.** Comparison of mRNA abundance changes (**RNA-seq**) with main coding sequence changes (**Ribo-seq**) of differentially expressed genes in UPF1 knockdown (**UPF1 KD**) cells.

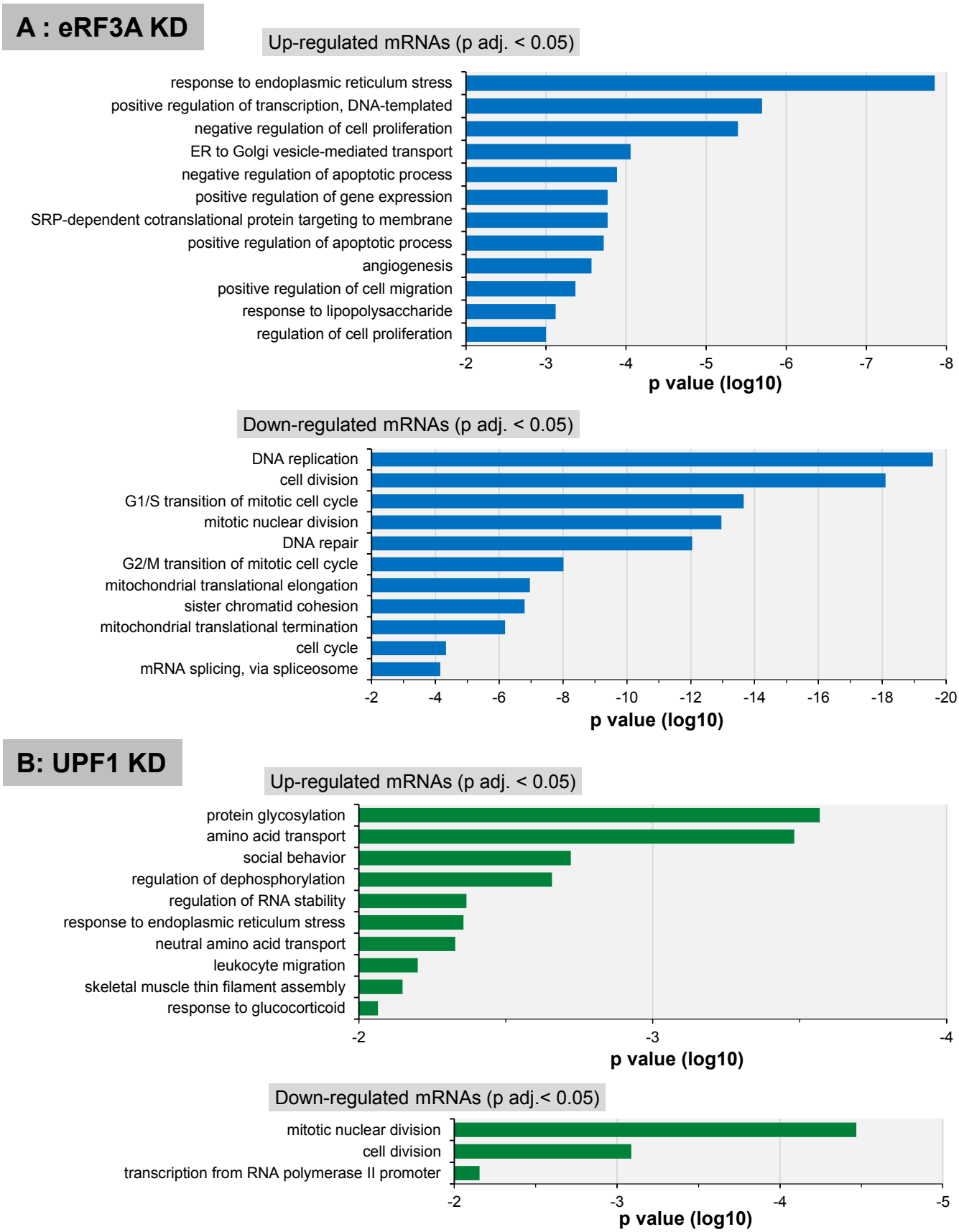

Supplemental Figure S4

Gene Ontology analysis. Biological process enrichment of differentially up-regulated or down-regulated mRNAs in eRF3a-depleted cells (eRF3A KD) **A.** and Upf1-depleted cells (UPF1 KD) **B.** Gene Ontology analysis was carried out using the DAVID gene ontology functional annotation tool (https://david.ncifcrf.gov/) with default parameters. We ranked terms according to the p-value.

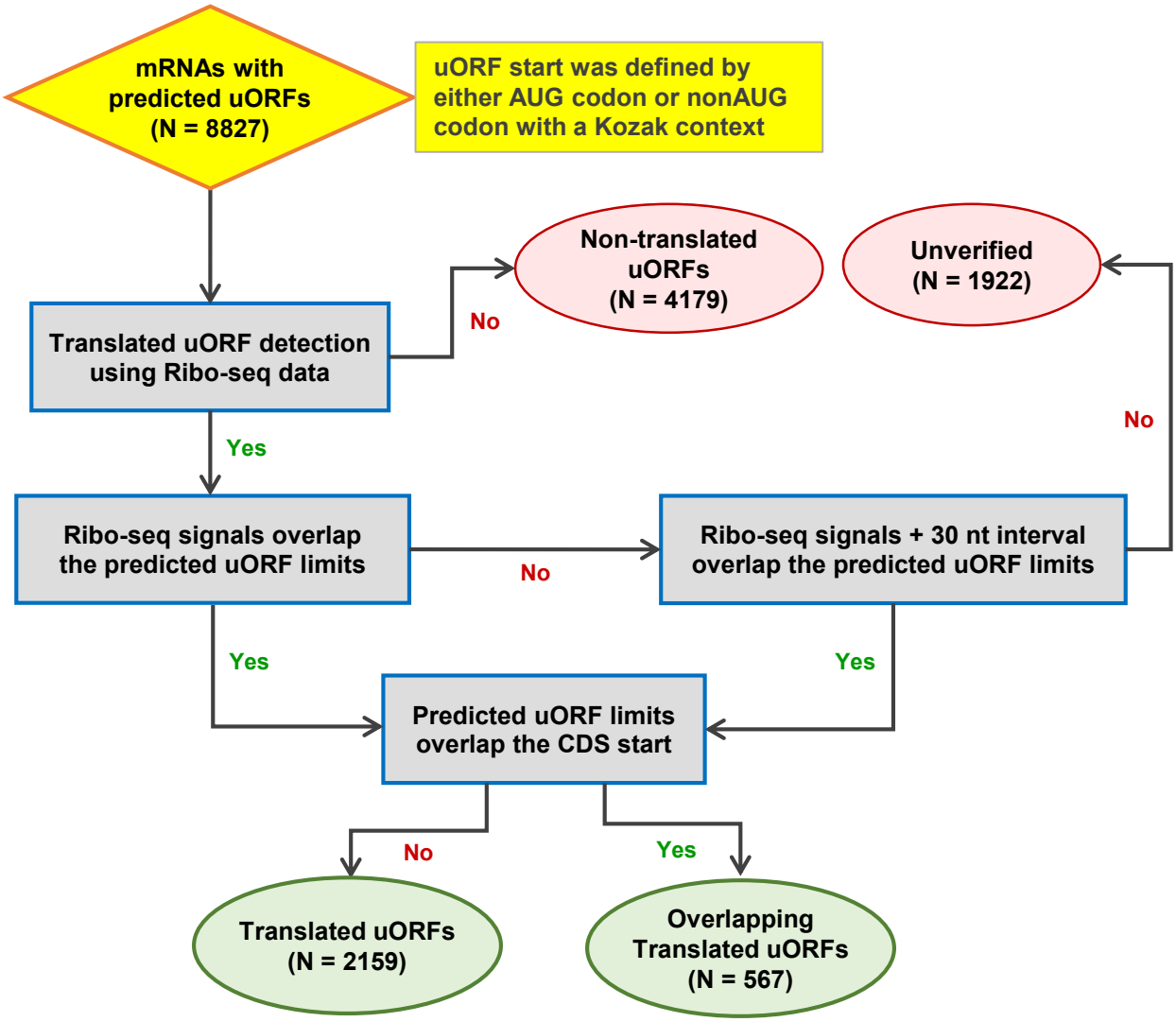

Supplemental Figure S5

Upstream openreading frame (uORF) detection in HCT116 transcriptome. Algorithm used for the detection of functional uORFs including those overlapping the main coding sequence (CDS) start site; the number of genes in each category is indicated. We first established a list of 8,827 genes with at least one predicted uORF in the human genome. The 4,179 Non-translated uORFs correspond either to transcripts that were not expressed in HCT116 cells or to the absence of ribosome footprint coverage in the region of the predicted uORF. The 1,922 transcripts noted "Unverified" correspond to Ribo-seq signals that could not be attributed to predicted uORFs. Kozak context (RCCNNNG, R = purine) is the optimal nucleotide context for translation initiation in mammals as defined by Marylin Kozak [46].

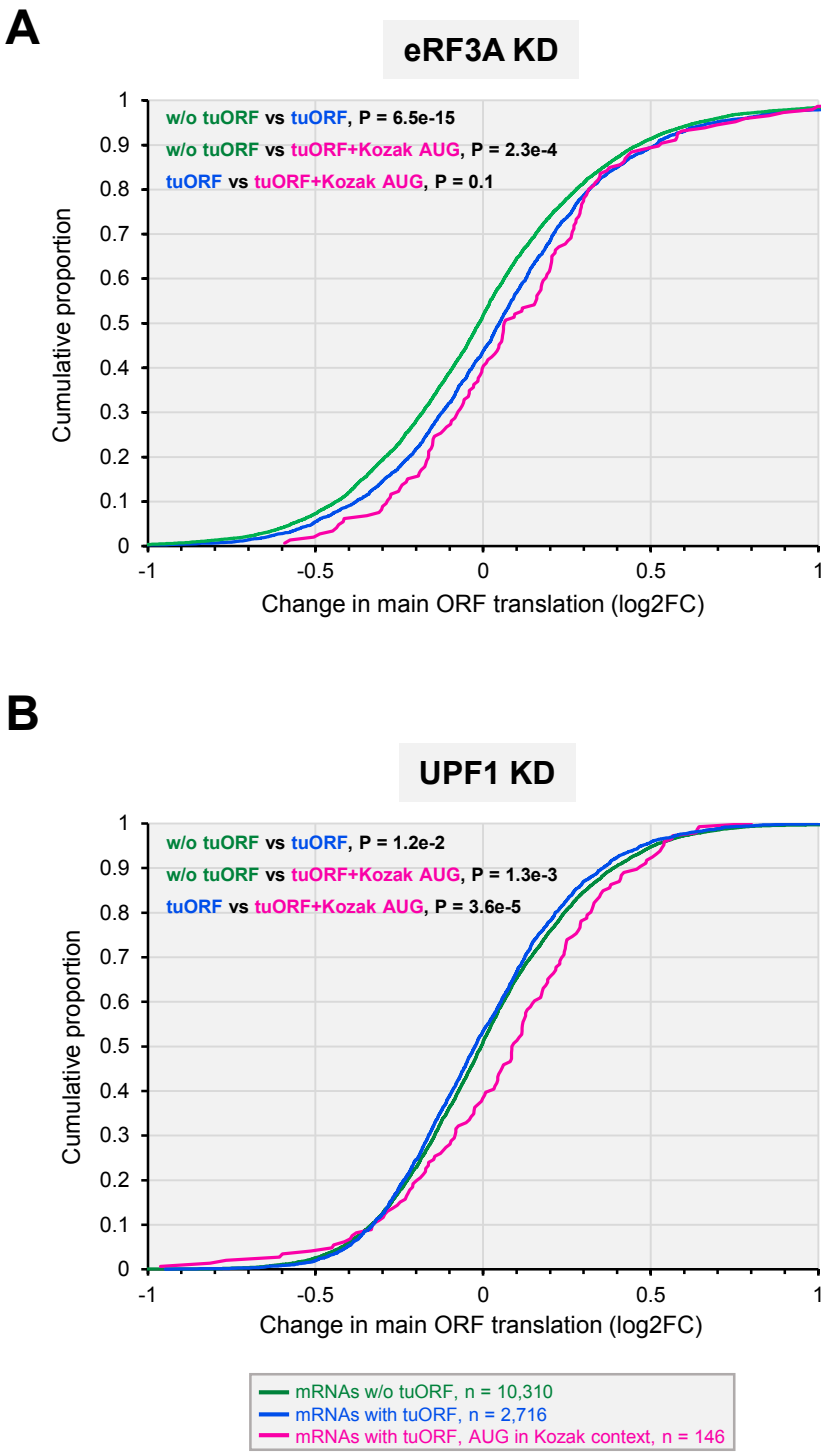

Supplemental Figure S6

Cumulative distribution functions of change in main ORF translation (plotted as log2FC) following either eRF3A depletion (**A**) or UPF1 depletion (**B**). mRNAs without translated uORF (**w/o tuORF, green line**), mRNAs with translated uORF (**tuORF, blue line**), mRNAs with translated uORF initiated by an AUG codon in a Kozak context (**tuORF, AUG in Kozak context, pink line**). P-values were determined by Wilcoxon rank sum test for the two sided hypothesis with a 95% confidence interval. The number of genes in each category is indicated below the graphs. mRNAs without translated uORF correspond to mRNAs devoid of uORF and to mRNAs with non-translated uORFs.

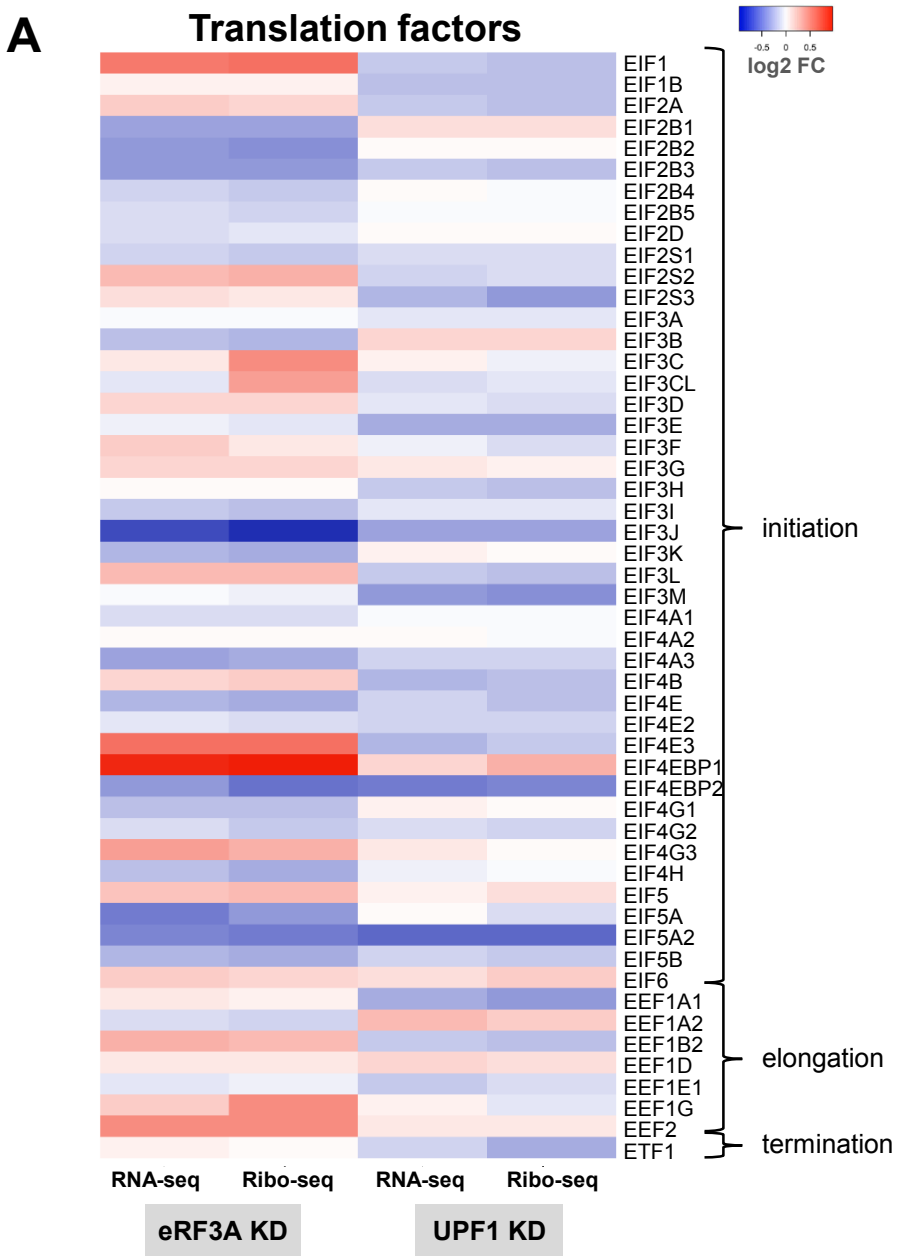

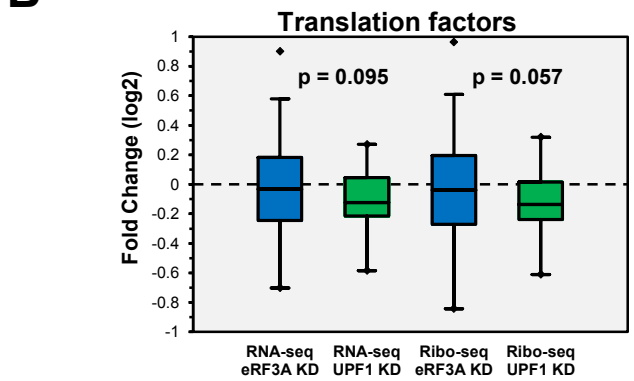

Supplemental Figure S7

A. Heat map representation of the differential expression levels (log2 FC scale) of the translation factor mRNAs in the transcriptome (**RNA-seq**) and translatome (**Ribo-seq**) following eRF3a knockdown (**eRF3A KD**) or Upf1 knockdown (**UPF1 KD**). Heat map was performed using Heatmapper website http://www2.heatmapper.ca/ without linkage clustering method. **B.** Corresponding box plot of log2FC values for translation factor mRNAs in RNA-seq and Ribo-seq experiments. The central lines show the medians; the box limits indicate the 25th and 75th percentiles. Two-tailed t-test was used to determine p-values.

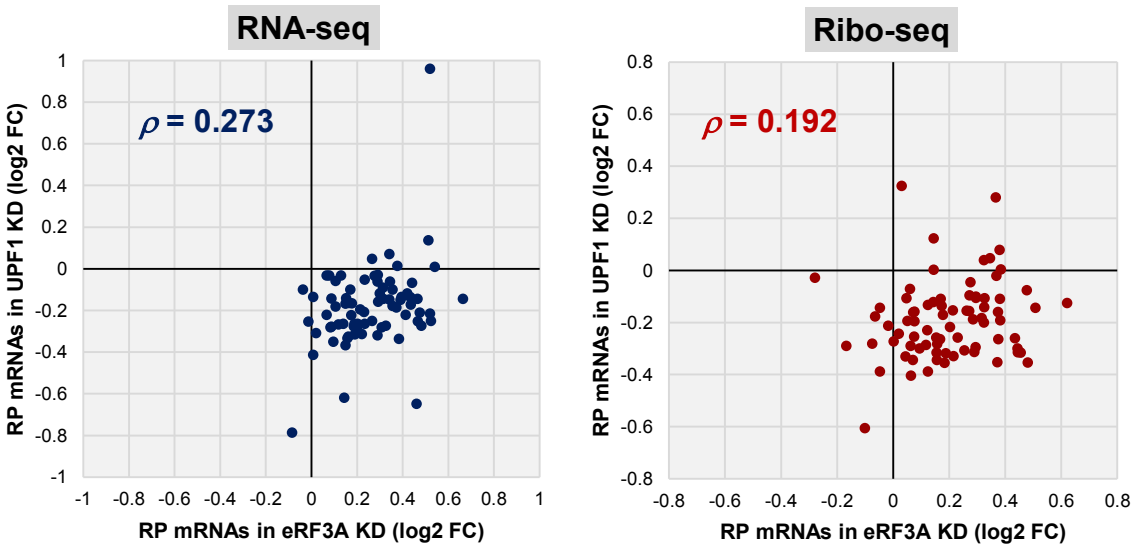

Supplemental Figure S8

Scatter plot of the differential expression of ribosome protein (RP) mRNAs in UPF1 knockdown versus eRF3A knockdown for RNA-seq (left panel) and Ribo-seq (right panel) data. All expression fold changes were plotted on a log2 scale. The Spearman correlation coefficient ρ is shown for each plot.

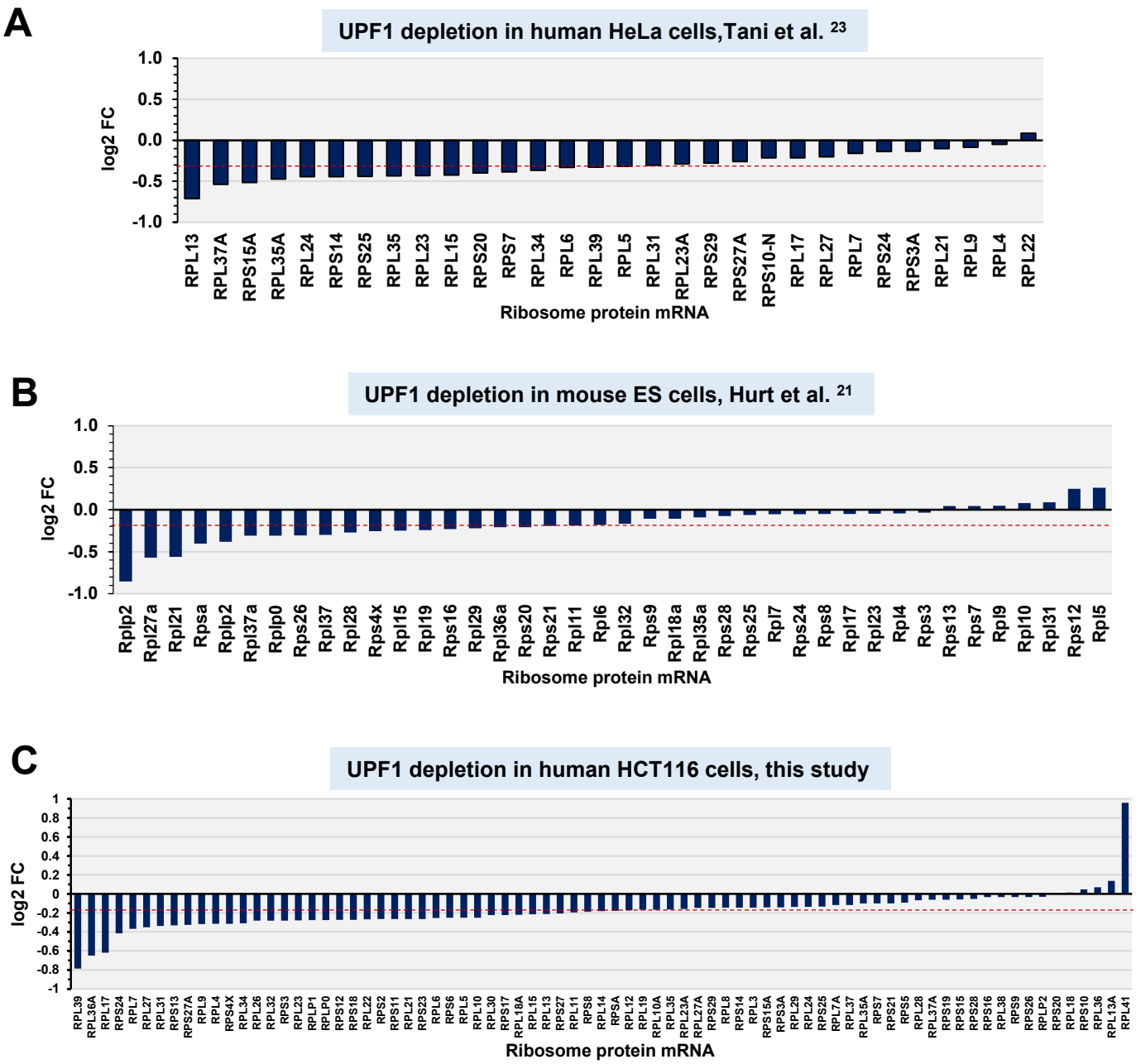

Supplemental Figure S9

Distribution of expression fold change (on a log2 scale) for ribosome protein mRNAs following UPF1 depletion (**A**) in human HeLa cells (Tani et al., 2012, ref. 23), (**B**) in mouse ES cells (Hurt et al., 2013, ref. 21) and (**C**) in human HCT116 cells (this study). Ribosome protein mRNAs were ranked from the smallest to the largest expression fold change. Red dotted lines represent the median value. Note that, for both studies,Tani et al. and Hurt et al., only incomplete sets of ribosome protein mRNAs were available in the supplemental files of the articles.